Available online at www.sciencedirect.com
ScienceDirect
Journal of the European Ceramic Society xxx (2008) xxx–xxx
www.elsevier.com/locate/jeurceramsoc

Time-resolved cathodoluminescence and photoluminescence of nanoscale oxides

L. Grigorjeva, D. Millers, A. Kalinko *, V. Pankratov, K. Smits

Institute of Solid State Physics, University of Latvia, Riga, Latvia

Abstract

The nanostructured oxide materials such as ZnO, ZrO_2, and $Y_3Al_5O_{12}$ (YAG) are perspective materials for transparent scintillating and/or laser ceramics. The luminescence properties of single crystals, nanopowders and ceramic were compared. Nominally pure and rare-earth doped nanopowders and ceramics have been studied by means of time-resolved luminescence spectroscopy.

The fast blue luminescence band was studied in ZnO ceramics sintering from different raw materials.

The luminescence centres of ZrO_2:Y were compared in a single crystal, ceramic and nanopowder.

It is shown that ceramic sintering parameters have a strong influence on time-resolved luminescence characteristics in cerium-doped YAG.

Keywords: Luminescence; Ceramic; ZnO; ZrO_2; YAG

1. Introduction

The range of optical ceramic application is extended significantly since the transparent ceramic was sintered. The ceramic materials have some advantages over single crystals: easy fabrication, lower cost, large homogenous samples, and possibility to doping without dopand segregation.

Ceramic materials were suggested for medical imaging in X-ray Computed Tomography.[1] The studies and developments of ceramic materials for detectors and scintillators are essential. Transparent ceramic materials with fast luminescence decay, low afterglow, high density (or radiation stopping power) and luminescence response in the visible region are required for technological applications. One of the promising materials for X- and γ-rays detection is ZnO. The density of ZnO (5.6 g/cm^3) is close to $(Y,Gd)_2O_3$:Eu, Pr ceramic (5.9 g/cm^3) used for medical imaging.[2] The luminescence of ZnO is in spectral region 3.35–3.1 eV at room temperature and the decay time was very fast (<1 ns).[3] The luminescence was attributed to radiative annihilation of different types of excitons and recombination of donor–acceptor pairs. Whereas the luminescence in ZnO crystal as well as in nanopowders was widely studied and models were discussed[4,5] the luminescence properties of ZnO ceramic are not reported. Note that ZnO ceramics synthesized from a powder precursor were studied mainly for varistor and sensor application.

The polycrystalline $Y_3Al_5O_{12}$ (YAG) ceramic doped with Nd is a known material for laser and scintillator application.[6] The main tasks for the laser ceramic is to reduce the light scattering losses and to obtain the higher doping level in comparison with YAG:Nd single crystal. The optical ceramic preparing techniques were successfully developed in past years.[7] The production of the transparent ceramic from YAG nanopowders has high importance. However, cerium-doped YAG ceramic and especially nanosized ceramic is poorly studied so far. Recently it was reported that transparent ceramic cerium-doped YAG samples were successfully sintered using nanosized powders as raw starting material.[8,9] Some of time-resolved luminescence properties of these nanosized ceramics are reported in the present study.

ZrO_2 (zirconia) is a widespread material due to large number of different applications, e.g., material for sensors,[10] solid electrolyte for fuel cells,[11,12] biocompatible material,[13] thermal coating barriers.[14] The luminescence of ZrO_2 ceramics was studied mainly for yttria-stabilized zirconia containing rare-earth dopands[15] and for mixed zirconia–aluminia ceramics.[16] The luminescence of zirconia ceramics was not studied in detail and the comparison of single crystal, ceramic and nanopowder luminescence could be fruitful.

* Corresponding author.
E-mail address: akalin@latnet.lv (A. Kalinko).

0955-2219/$ – see front matter © 2008 Elsevier Ltd. All rights reserved.
doi:10.1016/j.jeurceramsoc.2008.03.037

Please cite this article in press as: Grigorjeva, L., et al., Time-resolved cathodoluminescence and photoluminescence of nanoscale oxides, J. Eur. Ceram. Soc. (2008), doi:10.1016/j.jeurceramsoc.2008.03.037

However, the spectroscopic studies of rare-earth dopands in ceramic are scanty. In present paper we present the luminescence studies of YAG ceramic doped with Ce as well as ZnO and ZrO_2 ceramics. The results of time-resolved luminescence were compared for crystals, nanopowders and ceramic samples.

2. Experimental

For the cathodoluminescence excitation the pulsed electron beam was used. The electron beam has pulse duration 10 ns, fluency 10^{12} el/pulse and electron energy ~270 keV. The luminescence spectra were measured using grating monochromator (MDR-2) and photomultiplier tube. The output signal was displayed on the storage oscilloscope. The time resolution of a setup was 20 ns.

The photoluminescence spectra and decay kinetics were performed using pulsed laser excitation (4.66 eV, 8 ns) at room temperature. Luminescence registration carried out by photon counting head HAMAMATSU H8259 and photon counting board (fastComTec Communication Technology module P 7888-1E) with time resolution 2 ns.

The surface area (S_{BET}) was determined for all powders by BET method (Model Gemini 2360) using nitrogen as an adsorbate.

ZnO ceramic was sintered from different raw powders:

(a) *commercial ZnO powder* (*Aldrich 99.99; S_{BET} = 3.9 m^2/g, initial grain size 200–300 nm*). Sintering condition was: 48 h at the temperature 1400 °C in air. The average grain size in ceramic was ~10–15 μm;
(b) *ZnO nanopowder obtained by plasma technique*.[17] Powder characterization: S_{BET} = 22 m^2/g; nanowires structure; length 1–5 μm, diameter ~50 nm. The powder was mixed with 3% solution of oleic acid an alcohol. After being dried at 120 °C the powders were sieved through 200 μm sieve and pressed under the pressure of 1.0 MPa. The oleic acid was burn out at 650 °C and the pressed samples were sintered in air for 2 h at the temperature 1150 °C and the heating rate of 10°/min. Relative density of sintering ceramic was 96%. The average grain size was ~3 μm.

The ZrO_2:Y tetragonal structure single crystal was obtained from Alfa Aesar. ZrO_2:Y nanopowder was synthesized by hydrothermal method, nanocrystal structure was tetragonal, grain sizes within 13–27 nm. The luminescence properties of commercially available ZrO_2 ceramic were studied.

The cerium-doped YAG nanocrystals (powders) with a grain size of ~20 nm were obtained by the co-precipitation method. The peculiarities of the synthesis procedure are described in detail inRef. [18]. The phase structure of the nanopowders was controlled by X-ray diffraction analysis. The nanopowders obtained were used as raw starting materials for the synthesis of a nanostructured translucent ceramic.

The YAG nanoceramic samples were fabricated by means of a high pressure (up to 8 GPa) and low temperature (up to 450 °C) technique (see details inRef. [8]). The XRD analysis and SEM images were performed in order to compare the lattice structure and grain size of the starting nanopowders to the sintered nanoceramic samples. It was detected that fabrication process did not cause change in the structure and there was no significant grain growth.[8,9]

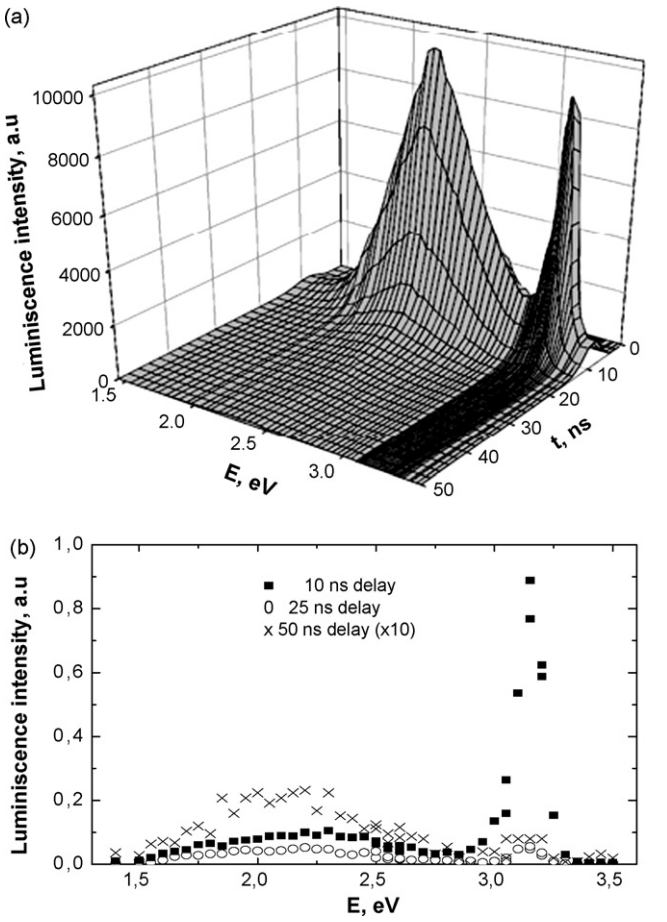

Fig. 1. Time-resolved luminescence spectra of ZnO ceramics: (a) from commercial powder, (photoluminescence) and (b) from powder obtained by plasma method (cathodoluminescence).

3. Results and discussion

3.1. ZnO ceramic

Time-resolved photoluminescence of ZnO ceramic (Fig. 1) shows the luminescence bands at 2.2–2.4 eV and 3.26 eV known for ZnO single crystals and nanopowders.[4] The luminescence mechanism of wide yellow-green emission is the recombination of defect states. The yellow (1.8–2.0 eV) luminescence was observed in cathodoluminescence spectra of nanopowders obtained by hydrothermal method.[19] The surface defect is involved in radiative recombination process in hydrothermal powder. In powders obtained by plasma method both 2.0 eV and 2.45 eV luminescence bands were detected. In commercial powder the defect luminescence was peaking at 2.45 eV. Luminescence band at 2.45 eV was observed in single crystal too and is ascribed as a recombination of native defect (single ionized oxygen vacancy) with photogenerated hole (Ref. [20] and references therein). In luminescence spectra of the ZnO ceramics

Please cite this article in press as: Grigorjeva, L., et al., Time-resolved cathodoluminescence and photoluminescence of nanoscale oxides, J. Eur. Ceram. Soc. (2008), doi:10.1016/j.jeurceramsoc.2008.03.037

obtained from commercial powder (Fig. 1a) the band is peaking at 2.45 eV whereas in ceramic sintered from plasma powder (Fig. 1b) the 2.0 eV and 2.45 eV bands were resolved. Thus the same defects states were in ceramic and raw powders though the ceramic sintering temperature is high (<1000 °C). Defect band luminescence decay was significantly faster in ceramic than that in ZnO single crystals and ZnO raw powders. The luminescence decay is not exponential. The decay rate estimation shows that the luminescence intensity falls to 10 times at first 150 ns in single crystal, 100 ns in nanopowders and at ~50 ns in ceramic. The afterglow level is low (<2% at 400 ns).

The fast blue luminescence peaking at 3.26 eV due to 1LO replica of free exciton was detected in photoluminescence spectra for ceramic obtained from commercial powder (Fig. 1a). In cathodoluminescence spectra the blue luminescence band peak position was shifted to 3.18 eV (Fig. 1b). This band was ascribed as luminescence due to exciton–exciton scattering and was detected under high density excitation.[4] One can note the intensity relation of defect band to exciton band is different in Fig. 1a and b. This difference could be due to various defect content as well as due to different excitation density. The luminescence decay is faster than our experimental equipment response (10 ns). The afterglow of blue luminescence is lower than 1% at 30 ns. The fast luminescence in blue spectral region was observed in all ZnO ceramic studied. An exciton-related luminescence mechanism in sintering ceramic depends on raw material used, sintering conditions and luminescence excitation density. Without doubt the ZnO ceramic is a promising fast scintillator material especially in the case of developing transparent ceramic sintering process.

3.2. ZrO_2 ceramic

Two kinds of ZrO_2 luminescence is known: (I) luminescence of self-trapped excitons[21] peaking within 4.2–4.4 eV and (II) intrinsic defects relating luminescence[22] covering spectral range ~1.5–3.5 eV. The luminescence of self-trapped excitons was observed below 150 K[21] and above this temperature the luminescence was quenched. Therefore at room temperature the self-trapped exciton luminescence is not observable. The peak position of defect luminescence is excitation wavelength dependent[22], indicating that a number of different defect types were responsible for luminescence observed. Our experiments were prepared at room temperature; therefore, only defect-related luminescence takes place. The irradiation with electron beam creates the band carriers; hence, the recombination process was responsible for luminescence centres excited states creation. During recombination all types of luminescence centres could be excited whereas a selective centre was excited by photo-excitation within band gap region.

The luminescence spectra of ZrO_2:Y single crystal, ceramic and nanopowder (nanocrystals) under electron beam excitation are shown in Fig. 2. One can find all three spectra were within ~1.5–3.75 eV. The origin of these wide spectra is emission overlapping from different luminescence centres. Some similarities in the spectra were found: single crystal and nanocrystals spectra were close to each other demonstrating that the recombination

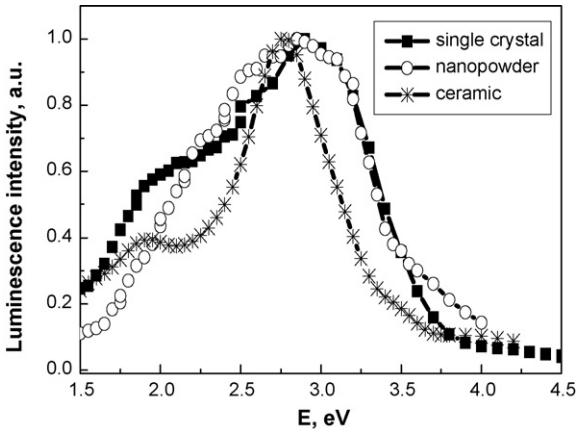

Fig. 2. Luminescence spectra of ZrO_2 single crystal, ceramic and nanopowder excited by electron beam at room temperature.

centres were similar also. In the ceramic spectrum, luminescence band is better resolved than in single crystal. Moreover, the spectrum of ceramic is narrower. It is surprising since due to disordered structure of ceramics one can expect more variety of defect types than in single crystal. On the other hand both single crystal and ceramic spectra reveal main maxima at ~2.8–2.9 eV and a shoulder at ~2.0 eV. This is evident that the main luminescence centres are similar. The differences could arise due to unexpected impurities incorporated in ceramic during sintering. These impurities obviously suppress some kind of luminescence centres and therefore relative contribution from other centres became more significant. Hence, the different contribution from various luminescence centres is the reason for differences in luminescence spectra of single crystal, ceramic and nanopowder. The main intrinsic defect in ZrO_2:Y is oxygen vacancy[23] and this vacancy could have three charge states: empty (V_0^{2+}), with one trapped electron (F^+-centre) and with two trapped electrons (F-centre). Besides charge state, the oxygen vacancy can have different positions relative to yttrium ions[22]; therefore, possible number of different luminescence centres seems to be large.

This is the ground for luminescence spectrum interpretation. Similar wide luminescence spectrum of tetragonal structure ZrO_2 nanopowders was observed by Wang et al.[24] This wide spectrum with poorly resolved structure was assumed to be from F^+-centres and centres including two oxygen vacancies. The two photoluminescence bands in ZrO_2:Y ceramics were described by Nakajima and Mori[25] and it was shown that the intensity of luminescence depends on Y_2O_3 concentration in the samples. Since the oxygen vacancy concentration also depends on Y_2O_3 concentration the conclusion was drawn out – origin of the luminescence are two kinds of oxygen vacancies – vacancies in the bulk and vacancies at the grain borders.

The wide luminescence spectra of ZrO_2:Y samples in our experiments were assumed oxygen vacancy related also. However really the spectra contain two kinds of bands: one wide structureless band and at least two narrow bands on the background of wide band mentioned. The wide structureless band seems to be dominant in nanopowder and it is assumed that the distorted zirconium–oxygen (Zr–O) complexes are responsible for this band. The distortion of Zr–O complexes arises due to

Please cite this article in press as: Grigorjeva, L., et al., Time-resolved cathodoluminescence and photoluminescence of nanoscale oxides, J. Eur. Ceram. Soc. (2008), doi:10.1016/j.jeurceramsoc.2008.03.037

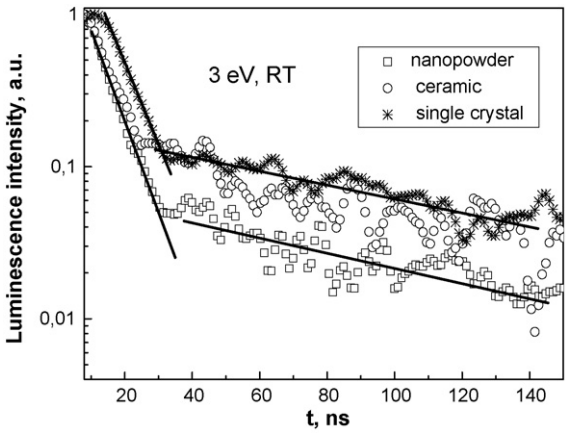

Fig. 3. Luminescence decay kinetics for ZrO_2:Y (Y_2O_3 concentration 6 mol%) single crystal, ceramic and nanopowder.

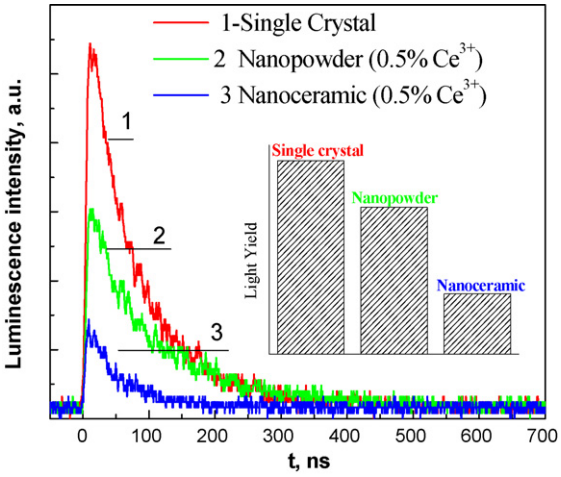

Fig. 4. Decay kinetic of cerium-related emission in YAG single crystal, nanopowder and nanoceramic under e-beam excitation. Luminescence light yield for each sample.

intrinsic defect (oxygen vacancy) and this distortion is different since it depends on Zr–O complex position relative to the oxygen vacancy. The narrow band origins from the Zr–O complex include the oxygen vacancy or from electron transitions in the defect (e.g. F^{+-} or F-centre). The model proposed predicts the luminescence decay kinetics can be similar for a single crystal, nanocrystals and ceramic since luminescence centres are similar. On the other hand, two kinds of luminescence centres (distorted Zr–O complex and Zr–O complex containing oxygen vacancy) and the luminescence bands of these centres overlap. Therefore the luminescence decay kinetics could have two components. The semi-logarithmic plot of luminescence decay kinetics is shown in Fig. 3.

The luminescence decay has the common feature—initial fast decay was followed by slower one. The largest contribution from fast decay was for nanocrystals. Contribution of fast and slow decay for single crystal and ceramic was close. In the terms of proposed model the contribution from distorted Zr–O complexes was larger for nanopowders; it is possible due to distortion of Zr–O complexes by surface defects also. Semi-logarithmic plot indicates the kinetics might be approximated by two exponents, thus two different excited states was.

3.3. YAG:Ce ceramic

The sintering processes may drastically change luminescence properties of the material. In fact, decay kinetics of cerium-related emission under electron beam excitation obtained for the single crystal, nanopowder (0.5% Ce^{3+}) and nanoceramic (0.5% Ce^{3+}) (Fig. 4) are different. Special experiment conditions were provided in order to compare light yield of luminescence for these three samples. Luminescence light yield in each case was determined as area under the corresponding decay curve and results were summarized on Fig. 4 inset. Noteworthy that cerium emission light yield is surprisingly low for the ceramic sample even comparing to raw starting nanopowder. For all nanoobjects studied (nanopowders and nanoceramics) decay kinetic of cerium-related emission can be approximated by the sum of two exponents with time constants τ_1 (fast component, ~20 ns) and τ_2 (slow component, ~70 ns), whereas decay kinetic of Ce^{3+} emission in a single crystal obeys the single exponential law with $\tau \approx 70$–80 ns. Cerium-related emission decay time constants τ_1 and τ_2 are very close for the nanoceramic and nanopowder samples; however, the contribution of fast and slow components is different.

The ratio of intensities of fast and slow components for the nanoceramic sample is about 5 and this value is approximately 5–6 times higher than for the nanopowder. Taking into account that grain size of nanoceramic is the same, as particle size of the nanopowder peculiar behavior of time-resolved luminescence characteristics in the nanoceramic would be explained in the framework of the model suggested in[26] for the nanopowders. This model suggests that there are two nonequivalent Ce^{3+} sites in nanopowders: "volume" and "surface". Therefore two components in the decay kinetics of cerium-related emission were detected: "volume" ions are responsible for the slow decay but "surface" ions for the fast one. Significant contribution of the fast component of the Ce^{3+} emission decay kinetic for the nanoceramic shows that the distribution of cerium ions was changed during the sintering process: impurity ions are "forced" from "volume" region to surface region, i.e. $Ce^{3+}{}_V$ ions diffuse to the surface forming $Ce^{3+}{}_S$. As a result Ce^{3+} ion concentration at grain boundaries becomes so high that concentration quenching appears. However, since nanoceramic was sintered at relatively low temperatures the diffusion of Ce^{3+} ions is highly unlikely. Therefore, obviously the change of the decay kinetic for nanoceramic is due to the high pressure applied. Most likely significant damages like dislocations are formed in the nanoceramic under high pressure. Since grain size of nanoceramics is relatively small (~20 nm) big dislocations may act as an "additional" surface and impurity segregation near dislocation lines likewise near grain surface is quite possible.

4. Conclusions

The fast blue luminescence band was observed in ZnO ceramics sintering from different raw materials. Since the decay time

Please cite this article in press as: Grigorjeva, L., et al., Time-resolved cathodoluminescence and photoluminescence of nanoscale oxides, J. Eur. Ceram. Soc. (2008), doi:10.1016/j.jeurceramsoc.2008.03.037

of this band is in subnanosecond region and low afterglow was detected the ZnO ceramic is a promising material for fast scintillator.

The luminescence centres of ZrO_2:Y are similar in the single crystal, ceramic and nanopowder. The two kinds of luminescence centres could be—distorted Zr–O complex and Zr–O complex containing oxygen vacancy. The distorted Zr–O complexes are proposed to be responsible for wide luminescence band in ZrO_2:Y. Zr–O complex containing oxygen vacancy account for narrow luminescence band appearing on the background of wide band mentioned. The differences of luminescence spectra of ZrO_2 single crystal, nanocrystals and ceramic are due to different contribution from two kinds of luminescence centres.

It was detected that ceramic sintering processes have a strong influence on time-resolved luminescence characteristics in cerium-doped YAG. A significant light yield degradation of cerium-related emission in YAG nanoceramic was observed and the mechanism responsible was suggested.

Acknowledgements

The authors wish to thank Prof. J. Grabis and Dr. T. Chudoba for supplying samples. This work was partly supported by Latvian Material Research Programme. V. Pankratov and K. Smits thank European Social Fund for the support.

References

1. Rossner, W., Bodinger, H., Leppert, J. and Grabmaier, B., The conversion of high energy radiation to visible light luminescent ceramics. *IEEE Trans. Nucl. Sci.*, 1993, **40**, 376–380.
2. Moses, W., Scintillator requirements for medical imaging. In *Proceedings of the 5th International Conference on Inorganic Scintillators and their Applications*, 1999, pp. 11–21.
3. Wilkinson, J., Ucer, K. B. and Williams, R. T., Picosecond excitonic luminescence in ZnO and other wide-gap semiconductors. *Radiat. Meas.*, 2004, **38**, 501–505.
4. Ozgur, U., Alivov, Y. I., Liu, C., Teke, A., Reshchikov, M. A., Dogan, S. *et al.*, A comprehensive review of ZnO materials and devices. *J. Appl. Phys.*, 2005, **98**, 041301.
5. Grigorjeva, L., Millers, D., Smits, K., Monty, C., Kouam, J. and El Mir, L., The luminescence properties of ZnO:Al nanopowders obtained by sol–gel, plasma and vaporization-condensation methods. *Solid State Phenom.*, 2007, **128**, 135–140.
6. Ikesue, A., Polycrystalline Nd:YAG ceramics lasers. *Opt. Mater.*, 2002, **19**, 183–187.
7. Taira, T., Ceramic YAG lasers. *CR Phys.*, 2007, **8**, 138–152.
8. Pązik, R., Głuchowski, P., Hreniak, D., Stręk, W., Roś, M., Fedyk, R. and Łojkowski, W., Fabrication and luminescence studies of Ce:$Y_3Al_5O_{12}$ transparent nanoceramic. *Opt. Mater.*, 2008, **30**, 714–718.
9. Chudoba, T., Teyssier, M. and Lojkowski, W., Optimization of conditions of preparation of YAG nanopowders for sintering of translucent ceramic. *Solid State Phenom.*, 2007, **128**, 41–46.
10. Figueroa, O. L., Lee, Ch., Akbar, S. A., Szabo, N. F., Trimboli, J. A., Dutta, P. K. *et al.*, Temperature controlled CO, CO_2, NO_X sensing in diesel engine exhaust stream. *Sens. Actuators B: Chem.*, 2005, **117**, 839–848.
11. Nguyen, N., Ceramic fuel cells. *J. Am. Ceram. Soc.*, 1993, **76**, 563–588.
12. Steele, B. C. H., Material science and engineering: the enabling technology for the commercialization of fuel cell systems. *J. Mater. Sci.*, 2001, **36**, 1053–1068.
13. Studart, A. R., Filser, F., Kocher, P. and Gauckler, L. J., In vitro lifetime of dental ceramics under cycling loading in water. *Biomaterials*, 2007, **28**, 2695–2705.
14. Zhou, H., Li, F., He, B., Wang, J. and deSun, B., Air plasma sprayed thermal barrier coatings on titanium alloy substrates. *Surf. Coat. Technol.*, 2007, **201**, 7360–7367.
15. Gutzov, S. and Lerch, M., Optical properties of europium containing zirconium oxynitrides. *Opt. Mater.*, 2003, **24**, 547–554.
16. Garcia, M. A., Paje, S. E. and Llopis, J., Luminescence of ZTA ceramics. *J. Lumin.*, 1997, **72-74**, 662–663.
17. Grabis, J., Šteins, I., Jankoviča, Dz., Dulmanis, A. and Heidemane, G., Preparation of nanosized oxide-based powders by gas and liquid phase methods. *Latv. J. Phys. Technol. Sci.*, 2006, **36**, 36–43.
18. Wang, H., Gao, L. and Niihara, K., Synthesis of nanoscaled yttrium aluminum garnet powder by co-precipitation method. *Mater. Sci. Eng. A*, 2000, **288**, 1–4.
19. Millers, D., Grigorjeva, L., Lojkowski, W. and Strachowski, T., Luminescence of ZnO nanopowders. *Radiat. Meas.*, 2004, **38**, 589–591.
20. Van Dijken, A., Meulenkamp, E. A., Vanmaekelbergh, D. and Meijerink, A., The luminescence of nanocrystalline ZnO particles: the mechanism of the ultraviolet and visible emission. *J. Lumin.*, 2000, **87–89**, 454–456.
21. Kirm, M., Aarik, J., Jurgens, M. and Sildos, I., Thin films of HfO_2 and ZrO_2 as potential scintillators. *Nucl. Instrum. Methods Phys. Res. A*, 2005, **537**, 251–255.
22. Petrik, N. G., Taylor, D. P. and Orlando, T. M., Laser-stimulated luminescence of yttria-stabilized cubic zirconia crystals. *J. Appl. Phys.*, 1999, **85**, 6770–6776.
23. Goff, J. P., Hayes, W., Hull, S., Hutchings, M. T. and Clausen, K. N., Defect structure of yttria-stabilized zirconia and its influence on ionic conductivity at elevated temperatures. *Phys. Rev. B*, 1999, **59**, 14202–14219.
24. Wang, Z., Yang, B., Fu, Z., Dong, W., Yang, Y. and Liu, W., UV-blue photoluminescence from ZrO_2 nanopowders prepared via glycine nitrate process. *Appl. Phys. A*, 2005, **81**, 691–694.
25. Nakajima, H. and Mori, T., Photoluminescence excitation bands corresponding to defect states due to oxygen vacancies in yttria-stabilized zirconia. *J. Alloys Compd.*, 2006, **408–412**, 728–731.
26. Pankratov, V., Grigorjeva, L., Millers, D., Chudoba, T., Fedyk, R. and Lojkowski, W., Time-resolved luminiscence characteristics of cerium doped YAG nanocrystals. *Solid State Phenom.*, 2007, **128**, 173–178.

Please cite this article in press as: Grigorjeva, L., et al., Time-resolved cathodoluminescence and photoluminescence of nanoscale oxides, J. Eur. Ceram. Soc. (2008), doi:10.1016/j.jeurceramsoc.2008.03.037